Conformational Analysis and Automated Receptor Docking of Selective Arylacetamide-Based κ-Opioid Agonists

Govindan Subramanian, M. Germana Paterlini, Dennis L. Larson, Philip S. Portoghese, and David M. Ferguson*

Department of Medicinal Chemistry and Minnesota Supercomputer Institute, University of Minnesota, Minneapolis, Minnesota 55455

Received May 20, 1998

The three-dimensional structure, dynamics, and binding modes of representative κ-opioid agonists of the arylacetamide class (U50,488; U69,593; U62,066; CI-977; ICI199,441; ICI197,067; BRL52,537; and BRL52,656) have been investigated using molecular modeling techniques. Systematic exploration of the conformational space of the ligand combined with molecular dynamics (MD) simulations in water revealed consistent conformational preferences for all the κ-agonists in this series. The results were further compared with available X-ray and 1D- and 2D-NMR data to identify potential "lead" conformers for molecular docking. Ligand binding modes were initially determined using automated docking of two of the ligands (U50,488 and BRL52,537) to the κ-opioid receptor. Extrapolation of the predicted binding mode to other members in this ligand series revealed similar docking preferences, with each ligand docked along the receptor helical axis. The binding modes were further refined using MD simulations of the receptor−ligand complexes. The results show a that salt bridge is formed between the amino proton of the ligands and the carboxylate group of Asp138 in TM3. This interaction most likely serves as a key anchoring point for the agonist association. Additional ligand contacts were noted with κ-specific residues Ile294, Leu295, and Ala298, which may, in part, explain the κ-selectivity in this series. In comparing the arylacetamides with opiate-based ligands, no evidence was found to link these classes through a common binding motif (except for the ion pair). The binding site model was also applied to explain the enantiomeric preference of U50,488 and to provide insight to the μ/κ-selectivity of representative ligands in this series. Overall, the results provide a structure-based rationale for ligand recognition that is consistent both with site-directed mutagenesis experiments and structure−function relationship data.

Introduction

The past decade has witnessed an upsurge in the development of highly selective, non-peptide ligands for the μ-, δ-, and κ-opioid receptors. While such compounds were developed as potential analgesics, they have applications as pharmacological tools as well.[1] Although a wide variety of opiate and opioid ligands have been described,[2] evidence has emerged for a unique class of highly selective κ-agonists based on the U50,-488 (**1**; Figure 1) structural prototype.[3] Representatives of this series (**1**−**10**) have been characterized as having several key features, including the arylacetamide moiety and a basic amino group as part of a pyrrolidine ring.[4] While some similarities can be drawn between **1**−**10** and opiate-based ligands, little evidence has surfaced to support comparative modeling of these ligand families. It is therefore not feasible to compare the binding modes or conformational preferences of **1**−**10** with opiates as molecular templates.[5,6]

Fortunately, some insights on the formation of **1**−**10** can be obtained from the structure−activity relationship (SAR) data for this ligand series. By varying the aryl (**1** vs **2**)[7,8] and amide (**1** vs **9**, **10**)[9−12] substituents, altering the chain length (spacer) between the aryl and amide group,[13] modifying the cyclohexyl moiety (**1** vs **3**−**8**),[14−19] and changing the ring size that contains the tertiary nitrogen, SAR studies have identified various means of optimizing the receptor−ligand interaction to improve the κ-opioid receptor binding and selectivity.[20,21] Although a simple spirotetrahydrofuranyl substituent on the cyclohexane ring in U50,488 [K_i(**1**) = 0.9 nM][22] reveals an increased ligand binding [K_i(**4**) = 0.3 nM],[15b] dramatic effects in the μ/κ-selectivity are observed when the aryl group is modified in concert.[7] Thus, CI-977 (**5**) displays greater selectivity (1575-fold)[7] for the κ-receptor as compared to **1** and **4** (280-fold).[15b] Likewise, SAR studies have demonstrated enantioselective binding for **5**,[8] with similar trends exhibited by other κ-agonists as well. Other interesting chemical modifications displaying selective κ-agonist activity are exemplified further by the ICI series (**6**−**8**)[17−19,23] and the piperidine derivatives (**9**, **10**).[9,10]

Despite these key developments in designing potent κ-agonists, the factors influencing the ligand binding and selectivity to the opioid receptors are not yet understood. Elucidation of the three-dimensional structure of the free ligand (**1**−**10**) and the receptor−ligand complex would afford a better understanding of the molecular recognition process at the κ-opioid receptor. In earlier work, we docked naltrexone-based compounds to a model-built κ-opioid receptor and illustrated the message−address concept of ligand recognition.[6] Our proposed receptor−ligand binding mode rationalized the observed point mutations and provided insights to the selectivity of naltrexone-based derivatives.[6] This recep-

10.1021/jm9803166 CCC: $15.00
Published on Web 10/28/1998

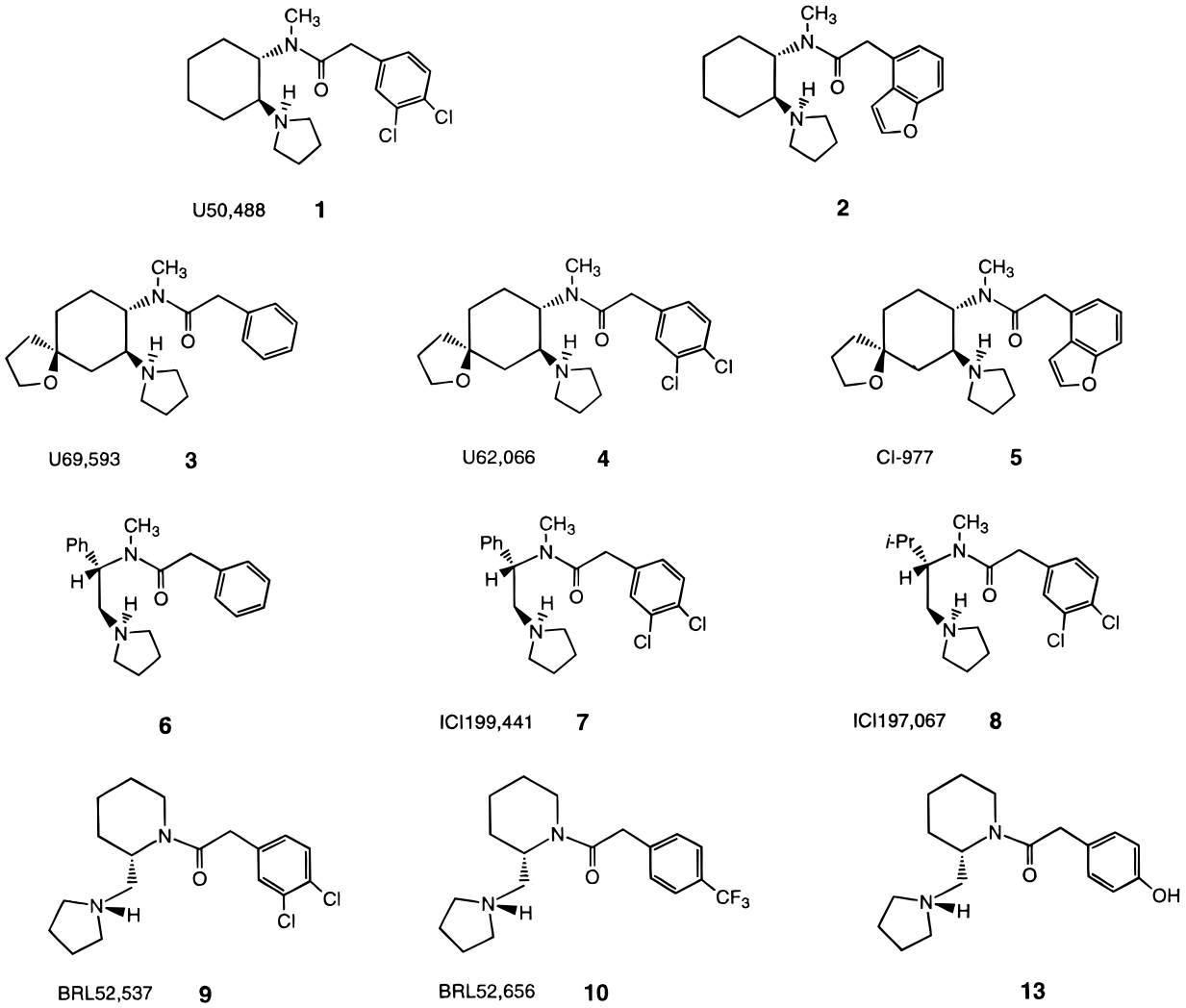

Figure 1. Structures of representative κ-agonists. All ligands carry a unit positive charge.

Table 1. Experimental Change in the κ-Binding Affinity (K_i(mut)/K_i(wild)) of **1**, **3**, **5**, and **6** for Specific Point Mutations

mutation	**1**[a]	**3**[a]	**5**[b]	**6**[b]
D105N	28.0	no binding	0.4	
T109A[c]			1.2	
Y119A[c]			1.9	
S123A[c]			0.6	
D138A	no binding[d]	no binding[d]	110.0	45.0
H291A			6.6	2.4
I294A			9.8	1.5
I294K			160.0	18.0
E297A			0.7	0.3
A298H			0.2	0.1
G319V			6.3	28.0

[a] Reference 25. [b] Reference 46. [c] Reference 26. [d] D138N mutation.

tor model has more recently been applied to explain the structural basis for dynorphin A binding and selectivity.[24] Herein, we extend a similar, but much more refined, computational approach in an effort to understand the three-dimensional structure, dynamics, and pharmacological features exhibited by the arylacetamide class of compounds (**1**−**10**), for which experimental site-directed mutagenesis results are rather limited (Table 1).[25,26]

Computational Methods

The crystal structures of **1**, **3**, and **7**[27] were used as starting ligand geometries, while the three-dimensional structures of **2**, **4**−**6**, and **8**−**10** (for which X-ray data are unavailable) were model-built by appropriate modification of closely related X-ray structures. The partial atomic charges for **1**−**10** were obtained from the multimolecular restrained electrostatic potential (RESP) charge fitting formalism[28] discussed in detail later. The initial geometry and charges thus obtained were subsequently used for in vacuo geometry optimization and energy minimization employing the steepest descent and conjugate gradient methods in the SANDER module of the AMBER 4.1 suite of programs.[29] All computations adopted the all-atom Cornell et al. force field[30] (*parm94.dat* of AMBER) which was modified to include the additional parameters listed in Table 2. A nonbonded cutoff of 8 Å was applied throughout, and the structures were considered energy-minimized when a convergence tolerance of 0.001 kcal/mol was met.

The conformational space of **1**−**10** was then explored using the SPASMS dihedral driver option with a distance-dependent dielectric of 4*r*. In addition, molecular dynamics (MD) simulations were employed to obtain detailed information on the most prominent local conformations of the free ligand. Accordingly, the in vacuo SANDER-optimized geometries (**1**−**10**) were placed in a periodic box of TIP3P water molecules.[31] After the geometry of the ligand was frozen, the solvent molecules alone were energy-minimized (20 000 cycles or 0.1 kcal/mol rms deviation in energy) and equilibrated for 5 ps in a constant temperature (300 K) bath. SANDER energy minimization (<0.01 kcal/mol rms deviation) and 2-ns MD simulation of the entire system followed this. SHAKE was used to constrain bonds involving hydrogen. A 1-fs time step was used along with a nonbonded cutoff of 8 Å at 1 atm of constant pressure.

Table 2. Additional AMBER Force-Field Parameters Used for κ-Agonists **1**−**10**[a]

bonds	K_b	R_0 (Å)
CA−CL[b]	244.6	1.719
CA−CW	546.0	1.352
CW−OA	427.0	1.351
CN−OA	428.0	1.350

angles	K_θ (kcal/mol/rad^2)	θ_0 (deg)
HC−CT−N[b]	30.2	109.0
CA−CT−C[b]	33.8	110.2
CA−CT−F[b]	46.8	109.0
CA−CA−CL[b]	39.6	118.8
CW−CA−HA	35.0	120.0
H4−CW−OA	35.0	120.0
H4−CW−CA	35.0	120.0
CA−CA−CW	63.0	120.0
CA−CA−CA	63.0	134.9
CB−CA−CW	63.0	106.4
CA−CW−OA	70.0	108.7
CA−CN−OA	70.0	132.8
CB−CN−OA	70.0	104.4
CN−OA−CW	70.0	111.6
CB−CA−CT	70.0	128.6
CA−CT−N	80.0	112.0

dihedrals	IDIVF[c]	K_ϕ (kcal/mol/rad)	phase (deg)	periodicity
CL−CA−CA−HA[b]	4	15.0	180.0	2
X −CW−OA−X	4	6.0	180.0	2
X −CW−OA−X	4	6.0	180.0	2
X −CA−CW−X	4	26.1	180.0	2

[a] Refer to text and ref 30 for atom definitions. [b] Derived from MM2-87 force fields. [c] Factor by which K_ϕ is divided.

The temperature was maintained at 300 K using Berendsen algorithm[32] with a coupling constant of 0.2 ps.

The receptor−ligand complex with a probable ligand binding orientation was built using various protocols and standard input options (as described in the DOCK manual) in the automated DOCK 3.5 suite of programs.[33] The receptor coordinates were taken from a model previously developed in our group to rationalize the binding of naltrexone-based derivatives[6] and dynorphin A(1−10).[24] Additional details regarding the receptor structure, site-directed mutagenesis data, and methods applied in developing the κ-model are available at our internet site (http://www.opioid.umn.edu). The model has also been compared with the recently published rhodopsin template of Baldwin.[34] Although slight differences in the orientation of the helices in the transmembrane (TM) domain are apparent, the juxtaposition of the residues within the putative binding pocket is well-conserved between the two models. The results reported here should therefore be transferable to other GPCR receptor structures with similar templates.

Since experimental mutagenesis (Table 1) and μ/κ-chimeric data[26,35] strongly suggest this ligand series is bound within the TM domain of the receptor, the extracellular loop structures were not considered here. The model-built TM helices[6] (excluding the hydrogen atoms) were used to create the solvent-accessible molecular surface (MS) employing the Connolly algorithm.[36] The program SPHGEN in DOCK 3.5 utilizes these points on the MS to generate spheres that fill the "putative binding pocket" in the receptor. However, the total number of spheres thus obtained was quite large (>225) and branched out to areas away from the putative "binding site". By visualizing all the spheres in the receptor using MIDAS 2.0 graphics utility program,[37] spheres that were away from the "binding pocket" were identified and removed manually from the sphere-cluster file. By this procedure, the number of spheres that act as a negative image and shape descriptor for the κ-agonists in the "binding pocket" was reduced to 84. Each sphere was assigned a close contact limiting distance of 1.3 and 1.8 Å for the polar and nonpolar

Chart 1

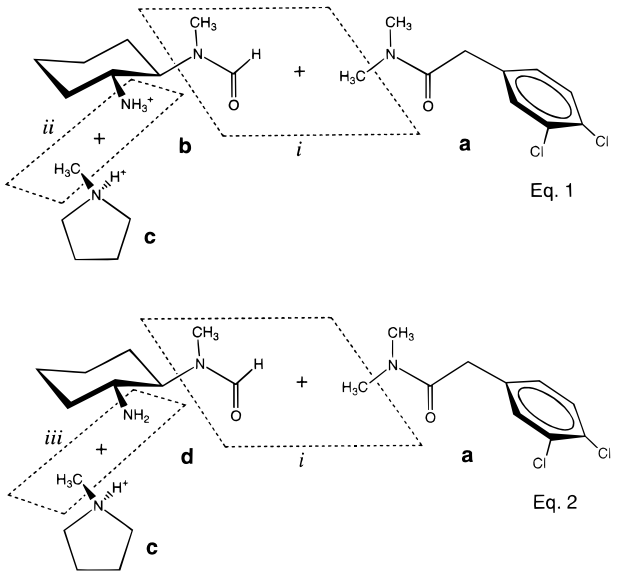

atoms, respectively. In addition, a cutoff distance of 4.5 Å for "good contacts" with the receptor was used.[33] The contact and force-field grids generated using the DISTMAP and CHEMGRID modules in DOCK 3.5 were used to score the different orientations of the ligand bound to the receptor. The force-field scoring (ffscore) that evaluates both steric and electrostatic contributions for each ligand binding orientation in the receptor was applied. The energy-minimized crystal structure of **1**[27a] was docked into the receptor "binding pocket" using the SINGLE mode in DOCK 3.5, and all possible binding orientations were searched. After identifying the most feasible receptor−ligand binding orientation (discussed later), the hydrogens were included to generate the tertiary structure of the complex.

Refinement of the receptor−ligand bound complex was achieved by in vacuo energy minimization using a distance-dependent dielectric function of $\epsilon = 4r$ and constraining the position of the backbone atoms using a force constant of 5 kcal/mol. The energy-minimized structure was then used as the starting point for subsequent 1-ns MD simulations, with the same backbone constraints as in the minimization step. A 1-fs time step was used, and the nonbonded pair list was updated every 25 fs. The temperature of the system was maintained at 300 K using the Berendsen algorithm with a 0.2-ps coupling constant.

Parametrization. RESP Charge Derivation: Computation of the electrostatic potential (ESP)-derived atomic charges for **1**−**10** using quantum mechanical approaches with reasonably large basis sets is quite expensive. Consequently, the κ-agonists were divided into smaller fragments that are suitable for ab initio calculations. The RESP charge-fitting formalism which derives the partial atomic charges of large molecules from the combined ESP of the fragments[38] was employed for **1**−**10**. For instance, U50,488 (**1**) was divided into three smaller fragments (*a*−*d*, Chart 1) without partitioning the amide bond. Since the pyrrolidine ring nitrogen is protonated in **1** and the fragmentation pattern involves the (sp^3)C−N(sp^3) bond cleavage, both the protonated (b; eq 1) and neutral (d; eq 2) amino substituents on the cyclohexyl fragment were considered. The HF/6-31G*-optimized geometries[39] and ESPs of the fragments obtained using the Gaussian94 program package[40] were utilized in the RESP charge-fitting procedure. The terminal blocking groups (*i*−*iii*, shown in dashed boxes in Chart 1) were then deleted to reassemble **1** from the fragments. The net charges of the blocking groups were distributed over all the fragments, while retaining the total molecular charge. As both fragments (b and c) are positively charged in eq 1, the dissociating group carries a unit positive charge ($q_i + q_{ii} = 1.0$), while the same is constrained to be neutral ($q_i + q_{iii} = 0$) in eq 2.

To assess the quality of the partial charges obtained from such fragmentation and recombination schemes, the RESP charges were also computed for **1** (crystal structure orientation)[27a] as a whole from the HF/6-31G*-optimized geometries and ESPs. A plot of the RESP atomic charges of U50,488 obtained from eqs 1 and 2 versus that for the whole molecule gives an excellent straight line fit with a correlation coefficient of 0.966 (eq 1) and 0.967 (eq 2). This clearly suggests that the RESP charges derived here do not depend on the choice of fragment (b or d) or on the fragmentation scheme (eq 1 or 2). Hence, the partial charges obtained from eq 2 were utilized for the MD and docking studies. In regard to the charges on the individual atoms, significant charge polarization is observed only for the carbonyl group (q_C = 0.588; q_O = −0.549), the proton on the basic nitrogen (q_H = 0.333), and the amide nitrogen (q_N = −0.274). This suggests the feasibility of direct electrostatic or ion-pair interaction of the proton on the sp^3 nitrogen with the electronegative or negatively charged substituents on the receptor. Notably, the sp^3 nitrogen (q_N = −0.078) and the chlorines (q_{Cl} = −0.102) do not bear appreciable charges. A similar fragmentation and reassociation strategy was extended to obtain the partial atomic charges of the other κ-agonists in this series (see Supporting Information). For example, *gem*-dimethyltetrahydrofuran and protonated *N*-ethylpyrrolidine fragments were used to compute the RESP charges for U62,066 relatives (**3**−**5**) and ICI derivatives (**6**−**8**). The pattern of the RESP atomic charges in **2**−**10** did not show any appreciable deviations when compared to **1**. It should however be mentioned that the sp^3 oxygen in the spiroether ring of **3**−**5** has a negative charge ($q_O \sim -0.465$) much greater than the sp^2 oxygen in the benzofuran ring ($q_O \sim -0.270$) of **2** and **5**.

Having built the electrostatic environment around the ligand, we incorporated the additional force-field parameters specific for **1**−**10** into the AMBER parameter file (*parm94.dat*).[29] Most of these parameters were either derived by analogy to existing AMBER potentials or derived from the MM2 force field[41] and are listed in Table 2. The stretching, bending, and torsional force constants along with the geometric parameters for the benzofuran ring in **2** and **5** were taken from the indole ring of tryptophan. However, the C−O distances were shortened by 0.03 Å from the corresponding C−N distances to account for the different electronegativities of the heteroatoms involved. The valence force constants for chlorine were adapted from the MM2 force field since no analogous parameter exist in AMBER. The nonbonded parameter for the sp^2 oxygen (OA; R^* = 1.74 Å and ϵ = 0.05 kcal/mol) in **2** and **5** was taken from MM2 (parametrized for furan). The nonbonded chlorine parameters (CL; R^* = 2.25 Å and ϵ = 0.2 kcal/mol) were reported by Veenstra et al.[42] The extension of the generalized AMBER torsional potentials in *parm94.dat* to such nonstandard molecules (**1**−**10**) was verified by comparing the computed in vacuo SPASMS[29] and ab initio relative energies of closely related U50,488 substructures, and the results are given in the Supporting Information.

Results

Conformational Space of κ-Agonists. Although the key structural features of U50,488 derivatives have been identified by SAR (Figure 1),[7−21] the conformational preferences of the free ligand or that involved in the receptor−ligand complex have not been investigated in detail.[23,43] In addition, the dynamic nature of the structure is of additional interest since there are many freely rotatable bonds in each molecule.

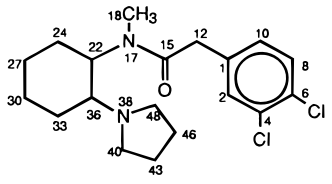

Table 3. Relative Energies (kcal/mol) and Torsional Angles[a] of SPASMS Geometry-Optimized U50,488 Conformers **1a**−**q**

no.	$[\theta_2,\theta_4,\theta_5]$	*RE*	no.	$[\theta_2,\theta_4,\theta_5]$	*RE*
1a	[174.2,−178.0,−50.5]	2.6	**1j**	[157.3,−17.4,−49.4]	4.0
1b	[−78.2, 176.8,−51.0]	0.0	**1k**	[−78.1,−11.4,−50.3]	3.5
1c	[70.6,−177.7,−50.4]	1.8	**1l**	[79.4,−10.2,−50.3]	0.5
1d	[−179.1,−175.1,165.0]	4.0	**1m**	[157.2,−10.4,163.0]	5.5
1e	[−89.4,−179.4,163.4]	1.1	**1n**	[−74.3,−6.8,163.5]	5.0
1f	[71.8,−177.9,164.9]	3.4	**1o**	[84.7,−5.8,163.2]	2.8
1g	[169.2,−172.7, 39.1]	4.5	**1p**	[152.0,−15.0,53.8]	5.3
1h	[−84.8, 177.6,50.5]	1.8	**1q**	[−72.1,−9.8,52.9]	5.0
1i	[68.9,−175.6,43.4]	3.7			

[a] Cis (∼0.0°); trans (∼180.0°); gauche$^-$ (∼−60.0° or 300.0°); gauche$^+$ (∼60.0°).

For instance, the three-dimensional structure of **1** is a function of the free rotations around the C^1-C^{12} (θ_1 = $C^2-C^1-C^{12}-C^{15}$), $C^{12}-C^{15}$ (θ_2 = $C^1-C^{12}-C^{15}-N^{17}$), $C^{15}-N^{17}$ (θ_3 = $C^{12}-C^{15}-N^{17}-C^{22}$), $N^{17}-C^{22}$ (θ_4 = $C^{18}-N^{17}-C^{22}-H^{23}$), and $C^{36}-N^{38}$ (θ_5 = $C^{22}-C^{36}-N^{38}-H^{39}$) bonds. The structural rigidity or flexibility depends on the barrier to rotation around these single bonds. Since pseudorotation of the five-membered ring may result only in small differences in energy and spatial arrangement, their contributions were not considered explicitly. Similarly, based on available NMR[43] and X-ray data,[27] the boat conformation of the cyclohexane moiety was ruled out. The flipping of the aryl group (θ_1) with two minima in the vicinity of ±90° is inconsequential as both conformers are supposedly equienergetic. This was demonstrated from HF/6-31G* calculations on the model compound, *N*-dimethyl-3,4-dichlorophenylacetamide, where the two stationary points corresponding to the 180° rotation of the aromatic ring possess an energy difference of only 0.3 kcal/mol. Likewise, extrapolation from known crystal structures (**1**, **3**, and **7**) indicates the $N-CH_3$ group aligns trans ($\theta_3 \sim 180°$) to the carbonyl group.[27] Hence the latter is considered as the rational choice for the amide orientation throughout this series (**1**−**10**).

Consequently, the conformational energy surface of the θ_2, θ_4, and θ_5 torsions alone were explored using the SPASMS driver routine in AMBER 4.1. Permuting all torsional combinations with 60° rotational increments of θ_2, θ_4, and θ_5 generated a total of 216 structures. Subsequent SPASMS energy minimization resulted in 17 structurally distinct conformers (Table 3). Inspection of these conformers revealed two rotameric domains (trans (*t*) = **1a**−**i** and cis (*c*) = **1j**−**q**) involving the amide nitrogen−cyclohexane bond (θ_4), while three minima are predicted for θ_2 (*t*, gauche$^+$ (g^+ or ∼60°), gauche$^-$(g^- or ∼−60°)) and θ_5 (*t*, g^+, g^-) for a given θ_4 torsion. Consistent conformational trends are discerned by the association of these different dihedrals and are referred to as $[\theta_2,\theta_4,\theta_5]$ in the discussion. The relative energies of the $-CH_2-$aryl orientation follow $[g^-,t,\theta_5] < [g^+,t,\theta_5] < [t,t,\theta_5]$ for a given θ_5 angle (for example, **1b** < **1c** < **1a**). However, the relative energy reorganizes as $[g^+,c,\theta_5] < [g^-,c,\theta_5] < [t,c,\theta_5]$ when θ_4 is in the vicinity of 0° (i.e., **1l** < **1k** < **1j**; Table 3). The gauche$^-$ and trans θ_2 dihedrals for trans θ_4 torsion are favored over the corresponding conformers for cis θ_4; the relative energies are $[g^-,t,\theta_5] < [g^-,c,\theta_5]$ or **1a**,**b** < **1j**,**k** as θ_5 is varied from gauche$^+$ (**1h** < **1q**) to trans (**1e** < **1n**) to gauche$^-$ (**1b** < **1k**). Except for **1l**, conformers with a cis θ_4 torsion (**1j**−**q**) are higher in energy than their corre-

sponding trans θ_4 forms (**1a**−**i**) and were therefore excluded from further consideration. Moreover, the X-ray structures of **1** and its relatives are illustrative of the trans θ_4 torsion (∼175°).[27a] Thus, among the remaining nine conformers (**1a**−**i**), the major difference relates to the orientation of the pyrrolidine ring with respect to cyclohexane (θ_5). Among these, conformers with a gauche$^-$ arrangement for θ_5 are relatively lower in energy than those with a trans θ_5 angle, for a similar θ_2 orientation (**1a** > **1d**, **1b** > **1e**, **1c** > **1f**). The most favorable conformer of U50,488 was indeed **1b** with a [g^-,t,g^-] arrangement and is 2.6 kcal/mol lower in energy compared to the X-ray structure orientation ([t,t,g^-], **1a**).[27a]

Although the relative energies of all nine isomers (**1a**−**i**) were within a few kcal/mol, the barrier to rotation around the C^{36}−N^{38} bond could lock the structure in one particular θ_5 torsion (preferably gauche$^-$). While crystal packing forces restrict the orientation of the aryl moiety (**1**) in the solid state, all the three θ_2 conformations (**1a**−**c**) could exist in dynamic equilibrium within the NMR time scale in solution.[43]

A similar strategy was extended to explore the conformational potential energy surface of other κ-agonists (**2**−**10**) as well. Since **2**−**5** differ mainly in the aryl modifications, the conformational profiles of [θ_2,θ_4,θ_5] torsion were similar to that of U50,488. However, subtle differences in the relative energies are noted especially for **4** and **5**, where the [g^+,c,g^-] torsion is predicted to be 0.3 and 0.7 kcal/mol more favored over the [g^-,t,g^-]. In contrast to **1**, the most favored arrangement of **3** possesses the same conformation ([g^-,t,g^-]) as that of the crystal structure.[27b] The conformational flexibility in **6**−**8** increases as a result of breaking the cyclohexane ring in **1** and introducing an ethyl linking group instead. This additional N(sp^2)−C(sp^3)−C(sp^3)−N(sp^3) torsion (θ_6) displays a significant preference for orientations around 60°, in addition to the [θ_2,t,g^-] dihedrals favored by the rotation of the other single bonds in **6**−**8**. Comparisons of the θ_6 torsion to similar environments in **1**−**5** (X-ray and low-energy SPASMS-generated conformers) also indicate that this angle is near 60°. Likewise, the piperidine derivatives **9** and **10** with a different type of cyclization also favor a 60° angle between the amide and basic nitrogens. Furthermore, all the SPASMS-optimized conformers obtained by permuting the [θ_2,θ_3,θ_5] angles in **9** and **10** revealed the amide nitrogen to be nearly planar and the piperidine ring to adopt a chair form. The conformational energy trends of **9** and **10** showed general agreement with that of **1**, with the low-energy structures possessing a gauche$^-$ (θ_5) arrangement.

Dynamic Properties of κ-Agonists. MD simulation techniques are used extensively to sample the conformational space and obtain structural details that cannot be elucidated from experiments. Apart from rationalizing the SPASMS results, this approach can provide a means of identifying the "static" versus "dynamic" nature of the θ_2−θ_6 torsions in the κ-ligands. Figure 2 shows the torsional trajectories of **1**, **3**, **5**, **7**, and **10** (refer to Supporting Information for other ligands) from a 2-ns simulation starting from the [t,t,g^-] orientations of the [θ_2,θ_4,θ_5] torsions. In general, the chair form of the cyclohexyl ring in **1**−**5** and that of the piperidine ring in **9** and **10** were the only ring puckers observed throughout the MD run. Similarly, the θ_4 torsion was arrested in the trans rotamer in **1**−**8**, while the θ_5 angle was confined to a gauche$^-$ arrangement in **1**−**3** and **10**, with the gauche$^+$ orientation (θ_5) sampled in addition for the remaining ligands. The pharmacophore torsion (θ_6) was locked in the gauche$^+$ form in **1**−**5** and **8**−**10**, but the flexible ethyl linker in **6** and **7** allowed for the population of trans (θ_6) dihedral arrangements as well. In fact, the strong conformational restriction of the θ_5 and θ_6 torsions in **1**−**10** resulted from the appropriate orientation of the N−H···O═C bond that maximizes the electrostatic interaction between the two moieties. The corresponding nonbonded distance from the MD simulations was 3.5−4.0 Å on average for most of the ligands.

Although the crystal structures (**1**, **3**, and **7**)[27] show the θ_2 torsion locked to a particular spatial arrangement, the MD simulations efficiently sampled all three θ_2 dihedrals in **1**, **3**, **4**, **6**, **7**, **9**, and **10**. However, bulkier aryl substitutions restricted the θ_2 torsion as evidenced from the simulation profile of **2** (vs **1**) and **5** (vs **4**). In general, the [g^+,t,g^-] orientation of the [θ_2,θ_4,θ_5] torsion is predicted to be the dominant solution conformation in **2**, **4**, **6**−**8**, and **10** and demonstrates that the most favored SPASMS-generated conformer ([g^-,t,g^-]) may not be the most populated in solution. This discrepancy between the MD simulations and conformational sampling (SPASMS) is likely due to the presence of explicit solvent (water) as opposed to the dielectric medium ($\epsilon = 4r$) used in SPASMS.

Apart from the presumed solvation effects, rotational barriers around single bonds (trans to cis θ_4 torsion in particular) also limit the population to only a few distinct conformers. For instance, the second most stable [g^+,c,g^-] conformer (**1l**) was not sampled in the 2-ns MD simulation of **1**. Similarly, the most favored SPASMS-generated [g^+,c,g^-] conformer of CI-977 (**5**) was not present in the 2-ns MD simulation but is consistent with the conformational sampling exhibited by the rest of molecules for the first 1-ns simulation. During the second 1-ns simulation, the structure became locked into the [g^-,t,g^+] orientation (Figure 2). Inspite of the sampling of some low-energy conformers (SPASMS) in the MD run, the simulations suggested that a large portion of each molecule (θ_4 in trans, θ_5 in gauche$^-$, and θ_6 in gauche$^+$) was anchored in space.

The substituted benzyl group (θ_2) of the κ-agonists adopted all three torsional degrees of freedom in solution. This was demonstrated by comparing the unique MD conformers of **1** ([θ_2,t,g^-]) with the conformations interpreted from experimental NMR data in D_2O (**1b**,**c**).[43] To accomplish this, the ^{1}H NMR chemical shifts of all three [θ_2,t,g^-] conformers, **1a**−**c** (Figure 3), with θ_2 torsional diversity were computed at the GIAO-Becke3LYP/6-31G*//HF/6-31G* level. In general, the protons of the cyclohexyl ring resonated upfield when compared to the pyrrolidine ring hydrogens. Similarly, the equatorial hydrogens (H_{eq}) of the cyclohexyl ring were downfield-shifted compared to the axial (H_{ax}) protons. In addition, these ^{1}H δ values were quite insensitive to θ_2 torsions (refer to Supporting Information for the computed chemical shifts). However, the subtle yet significant differences in the aromatic, ben-

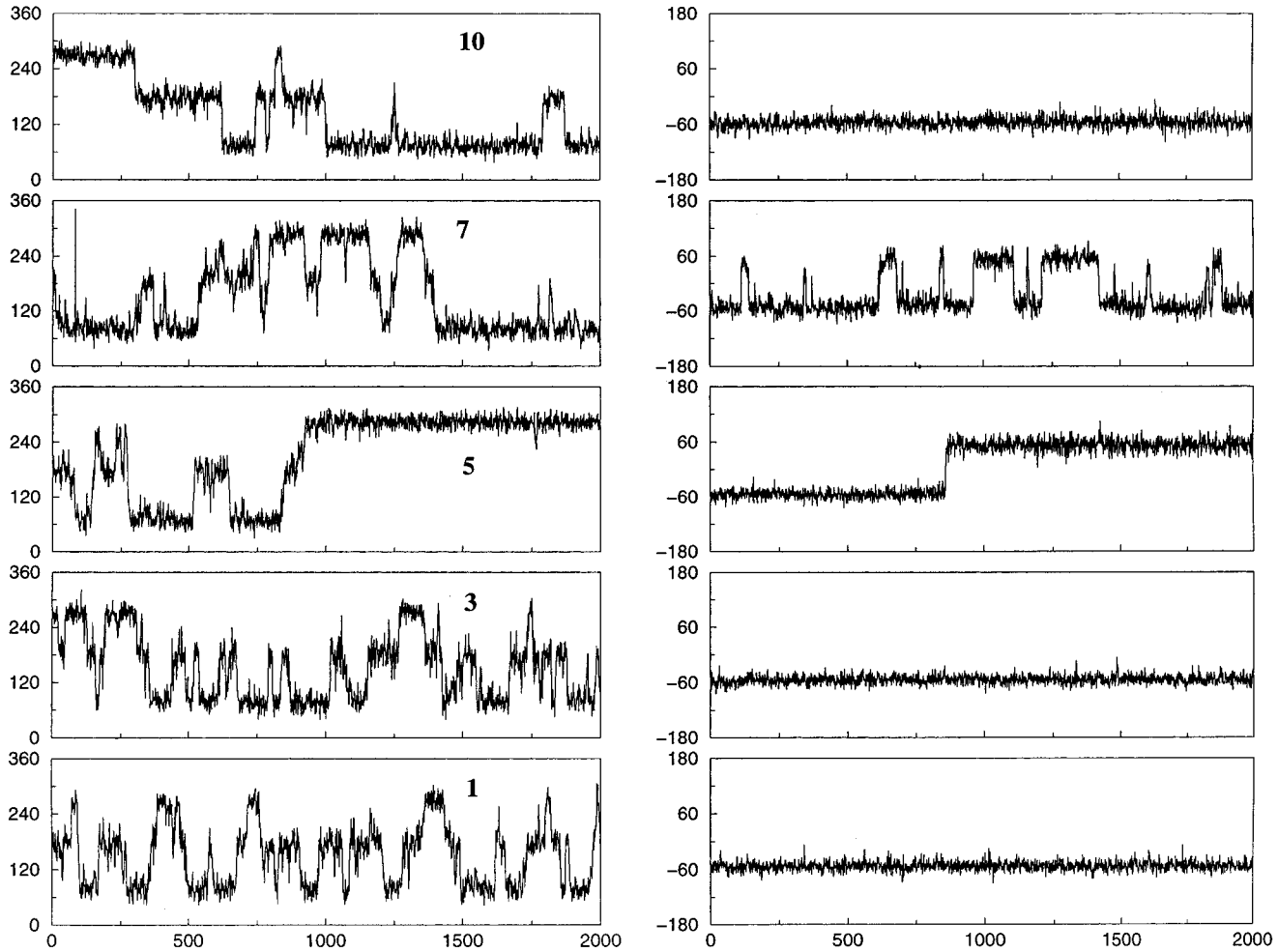

Figure 2. θ_2 (left) and θ_5 (right) torsional profile of the solvated ligands as a function of MD simulation time (in ps). The ligand numbers are given in each graph.

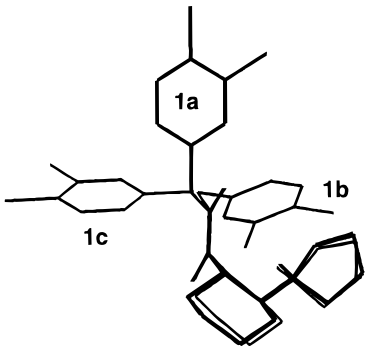

Figure 3. Superimposed in vacuo SPASMS geometry-optimized structures **1a**−**c**.

Table 4. GIAO-Becke3LYP/6-31G*//HF/6-31G*-Computed ^{1}H NMR Chemical Shifts (δ, ppm) for U50,488 Conformers **1a**−**c**[a]

atom no.	δ **1a**	δ **1b**	δ **1c**	δ_a **1a**−**c**	expt
H3	6.9	7.0	7.1	7.0	6.8
H9	7.3	7.3	7.3	7.3	7.2
H11	6.7	7.4	6.8	7.0	7.1
H13	3.3	3.2	3.8		
H14	3.3	3.7	3.3	3.5	3.5
H19	2.5	3.3	2.5		
H20	2.8	2.9	2.3	2.7	2.7
H21	2.9	3.0	2.7		

[a] The average chemical shifts (δ_a, ppm) and the experimental values (ppm) are given for comparison. The computed and experimental ^{1}H δ values for the cyclohexyl and pyrrolidine rings are given in the Supporting Information.

zylic methylene, and *N*-methyl δ ^{1}H values are a consequence of the different θ_2 torsions (Table 4). Although, the experimental assignments suggested the existence of **1b**,**c** alone in solution,[43] our interpretations of the chemical shifts include the coexistence of the crystal structure orientation (**1a**) as well. Thus, the average ^{1}H NMR shifts (δ_a) of **1a**−**c** are in better agreement with the experimental values[43] than any one single conformer (**1a**−**c**), thereby supporting the highly fluxional behavior of the θ_2 torsion within the NMR time scale.

Automated Docking of Agonists in the κ-Receptor. Identification of the bioactive conformation from the pool of possible conformers (Table 3) is a critical issue in predicting the appropriate ligand binding mode. Even though the MD simulations simplified the number of possible ligand conformers to just three [θ_2,t,g^-] structures, only one among them was anticipated to be the dominant binding conformer. Experimental SAR

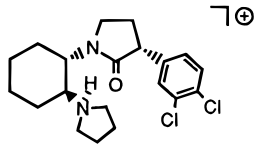

11

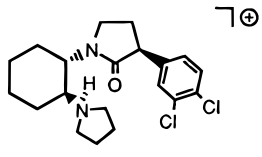

12

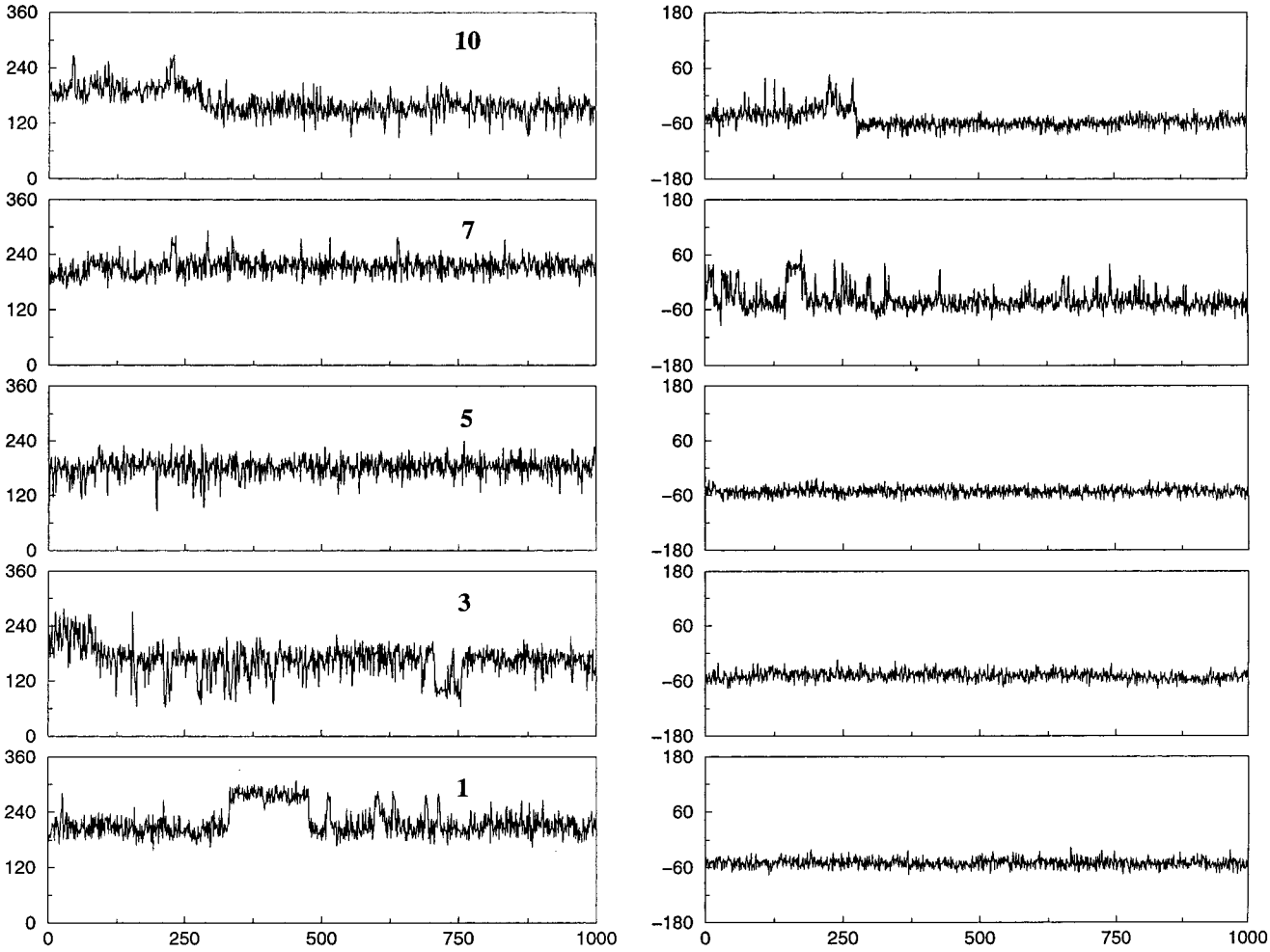

Figure 4. θ_2 (left) and θ_5 (right) torsional profile of the docked ligand as a function of MD simulation time (in ps). The ligand numbers are given in each graph.

studies on racemic U50,488 and its constrained lactam analogues[44] (**11**, **12**; note that the θ_2 torsion is restrained) revealed the binding (K_i) to be similar for **1** (15.0 nM) and **11** (10.0 nM), but 6−9-fold lower for **12** (92.0 nM) indicating the effects of the θ_2 torsion on binding. This tentatively justifies the [*t*,*t*,*g*$^-$] orientation as a reasonable starting structure that could be docked to the κ-receptor. Although there are various possibilities of docking these flexible ligands to the receptor, finding the favorable low-energy states in the receptor-binding domain is often tedious. Consequently, we employed the automated DOCK program to explore the possible orientations of U50,488 (**1a**) within the receptor binding pocket. Accordingly, the "best positions" for the ligand atoms, and thereby the ligand recognition sites, were identified by searching for regions of complementarity within the TM helices.[45] Out of the 982 configurations generated by DOCK, the top-ranking 107 orientations that were within 5 kcal/mol from the best force-field score (ffscore = −29.5 kcal/mol) were extracted. Interestingly, all the binding orientations of **1a** were along the receptor helical axis (positioned vertically) and none perpendicular to it (horizontal). In addition, the DOCK search suggested the aryl group in U50,488 to be either toward the extracellular region or deep in the binding pocket.

The tentative ligand binding domain predicted by the automated docking procedure also suggested the putative ligand binding pocket to comprise TM3, -5, -6, and -7.[45] Preliminary analysis of the docked structures indicated that the best and many of the top-scoring structures had the pyrrolidine ring aligned near E297 (TM6) of the κ-receptor (the aryl group is down in the pocket; see Supporting Information), while few structures had this moiety close to H291. Nevertheless, the complete loss of U50,488 binding[25] upon a D138N (TM3) mutation suggests the ion pairing between the protonated nitrogen of **1a** and the D138 carboxylate group is a key binding interaction. A closer examination of some of the top-scoring orientations identified the 31st best-docked configuration of **1a** (ffscore = −24.8 kcal/mol) as having the basic nitrogen close to D138 in TM3 and the aryl group tethering toward the extracellular region. Although this arrangement would have been expected to be the top-scoring orientation, short-range steric conflicts between the receptor side chains and the ligand resulted in this binding arrangement having a lower scoring. This was evident when the energy components of the force-field score between the 31st and the best-docked configurations were compared. The electrostatic and the van der Waals (vdW) attraction energies (kcal/mol) were better stabilizing for the 31st best-docked structure (−3.9, −44.6) as compared to the top-scoring orientation (−3.2, −39.5). However, the corresponding contribution from the vdW repulsion (23.8, 13.1) reversed the *numerical* preference of the force-field scoring

Table 5. Average Distances (dist, Å) of the Free and Receptor-Bound Ligands **1**−**10** Obtained from MD Simulations

param	**1**	**2**	**3**	**4**	**5**	**6**	**7**	**8**	**9**	**10**
dist1[a]	4.169	3.961	3.936	3.944	4.196	5.900	4.319	4.366	5.029	3.274
dist2[b]	4.270	3.969	3.985	3.960	4.183	5.966	4.381	4.340	4.706	3.215
dist3[c]	7.362	7.408	10.590	10.080	8.885	4.913	5.042	6.336	6.855	9.490
dist4[d]	5.383	5.534	8.246	7.613	7.014	4.206	3.879	4.435	5.393	7.261
dist5[e]			5.933	6.991	5.848					
dist6[f]			4.097	5.159	3.939					
dist7[g]	6.106	7.117	10.234	8.370	6.950	6.737	7.589	7.303	11.250	10.481
dist8[h]	6.021	7.119	10.263	8.748	7.149	6.671	7.643	7.085	11.622	10.455

[a] (D138-carboxyl oxygen)O^1···H−N(ligand) distance. [b] (D138-carboxyl oxygen)O^2···H−N(ligand) distance. [c] (H291)δN−H···O=C(ligand) distance. [d] (H291)ϵN···O=C(ligand) distance. [e] (H291)δN−H···O(sp^3)(ligand) distance. [f] (H291)ϵN···O(sp^3)(ligand) distance. [g] (E297-carboxyl oxygen)O^1···C^{para}(aromatic, ligand) distance. [h] (E297-carboxyl oxygen)O^2···C^{para}(aromatic, ligand) distance.

for these two docked configurations. This clearly emphasizes the limitation of rigid docking methods and cautions against blindly choosing the best force-field-scoring configuration always as the ideal ligand binding mode in the receptor. In fact, it is necessary to closely examine some of the top-ranking distinct configurations of the ligand in the receptor before concluding on the most relevant bound complex.

Instead of extending the DOCK protocol to predict the binding domain of **2**−**8**, their structural and spatial similarity were taken to our advantage. The direct relationship of the preferred torsions of **2**−**8** with U50,-488 suggested that they might also exhibit similar binding characteristics in the κ-receptor. The comparable κ-affinity of **1**−**10**[8,10,13,15,17,20,23] and the impairment of U69,593, CI-977, and ICI199,441 binding upon a D138 mutation (Table 1)[25,46] provided support for our claim of binding complementarity. Consequently, the [t,t,g^-] SANDER energy-minimized structures of **2**−**8** were superimposed on the docked structure of **1a** (31st configuration)[47] to generate the tertiary structure of the receptor−ligand complex. Since **9** and **10** possessed a piperidine ring, the complete DOCK procedure was followed to obtain their probable binding orientation (the [t,t,g^-] conformations of the ligands were considered). A strategy similar to that used for **1a** was employed to retrieve the binding mode of **9** where the pyrrolidine ring was closer to the D138 residue of the receptor. Overlapping **10** on the docked configuration of **9** generated the receptor−ligand complex of **10**.

Having established the most likely binding mode of **1**−**10**, post-DOCK refinements (energy minimization and MD simulations) were employed to relieve any steric conflicts between the flexible amino acid side chains of the receptor and the docked ligand. A comparison of the MD trajectories of the free ligand (Figure 2) and the bound complex (Figure 4) indicates that the ligand conformer in the receptor is not the most favored or highly populated solution structure in some cases. As in the free ligand, the θ_5 torsion in **1**−**5** and **10** bound to the receptor was locked in the gauche$^-$ form with occasional transitions to the trans and gauche$^+$ rotamers for **7**−**9** (Figure 4 and Supporting Information). However, the gauche$^-$ arrangement was the most populated θ_5 torsion in all the docked ligands. Similarly, the dominant θ_2 torsions were close to the trans in a majority of ligands (**1**−**3**, **5**−**7**) associated with the receptor, while the gauche$^-$ orientation seem to be favored for **8** and **9**. Interestingly, U62,066 (**4**) exhibited θ_2 torsional phase transition from trans to gauche$^+$ after 300 ps. There is also evidence that the X-ray structure is not necessarily the bound conformation. This is demonstrated by considering the energy-minimized crystal structure orientation of U69,593 (**3**, [g^-,t,g^-])[27b] as a starting ligand conformer. The initial receptor−ligand complex was built by overlapping **3** on the U50,-488 docked structure (31st configuration) and following the minimization and MD protocols similar to that employed for other bound ligand complexes. In less than 100 ps of the 1-ns simulation, the θ_2 torsion (see Supporting Information) of U69,593 converted back to the preferred trans form (and θ_5 = gauche$^-$), suggesting that the MD run here was not dependent on the initial θ_2 ligand torsion. In general, the ensemble of conformers for each ligand generated from the simulation of the complex implicated the [t,t,g^-] torsion as the dominant binding orientation for **1**−**3**, **5**−**7**, and **10**. However, the [g^-,t,g^-] is favored for **8** and **9**, with U62,066 (**4**) alone adopting the [g^+,t,g^-] arrangement in the receptor. It should however be emphasized that a single conformational element (frozen ligand orientation) does not exist for the receptor−ligand complex (Figure 4), and any insights gained from static energy minimization of the complex need to be treated with caution.

Discussion

As mentioned earlier, the carboxylate group of the aspartate (D138) in the κ-receptor located in TM3 is presumed to form a salt bridge with the pyrrolidine ring amino proton of the ligands.[26,45] The notion that D138 in the κ-receptor is involved in direct ligand recognition has also been suggested from site-directed mutagenesis in which a D138N mutation abolishes U50,488 and U69,593 binding.[25] Likewise, the D138A receptor mutation impaired CI-977 and ICI199,441 association significantly.[46] Owing to alike structural and spatial relationships of **1**−**10**, it is reasonable to speculate that D138 serves as a common interaction point for other κ-agonists in this series. Accordingly, MD simulations of all the bound ligand complexes resulted in the protonated nitrogen forming a sustained salt bridge with the carboxylate group of D138 (Table 5). The carboxylate oxygen to the pyrrolidine proton distance was 3.9−4.3 Å on an average for most of the ligands (Table 5) and is within the anticipated range for similar salt bridges.[48] In fact, such direct electrostatic anchoring of the ligand moiety with the aspartate most likely causes the remaining portion of the agonist to reorganize by taking advantage of the surrounding receptor environment (Figures 5 and 6).

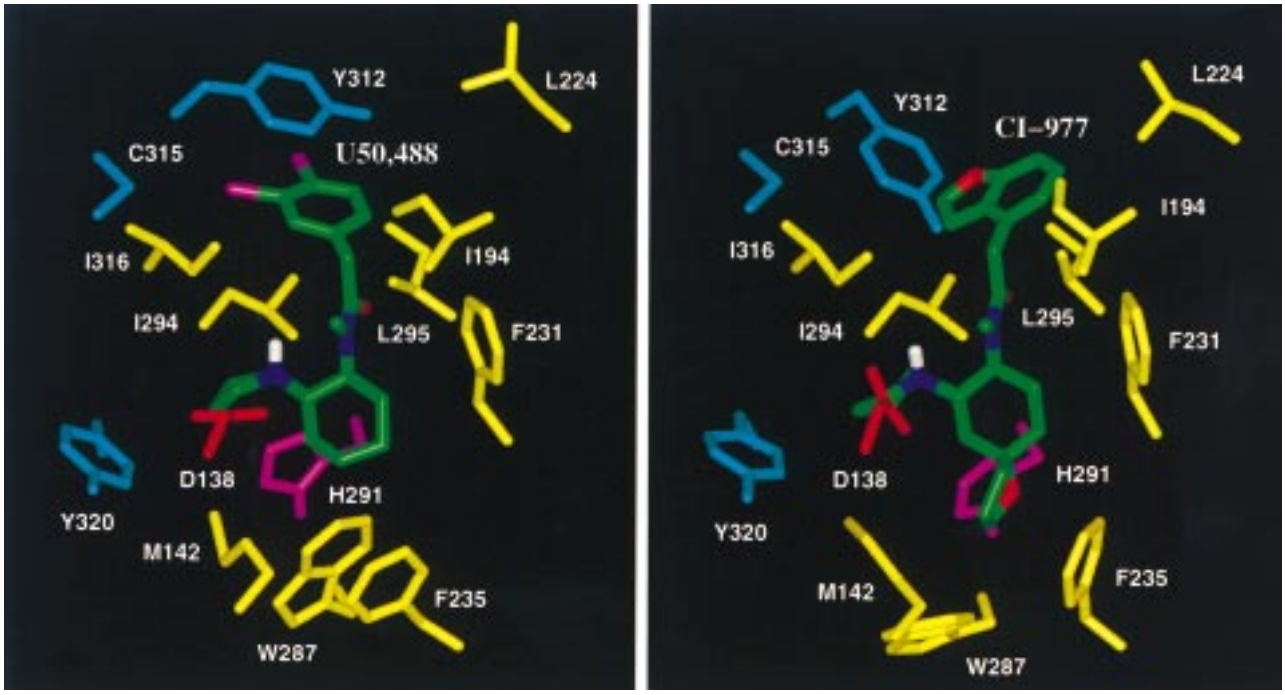

Figure 5. Molecular dynamics snapshot of U50,488−receptor (left) and CI-977−receptor (right) complexes. Selected residues that are within 5 Å from the ligands are shown as follows: D138 in red, polar residues in cyan, hydrophobic residues in yellow, and H291 in magenta.

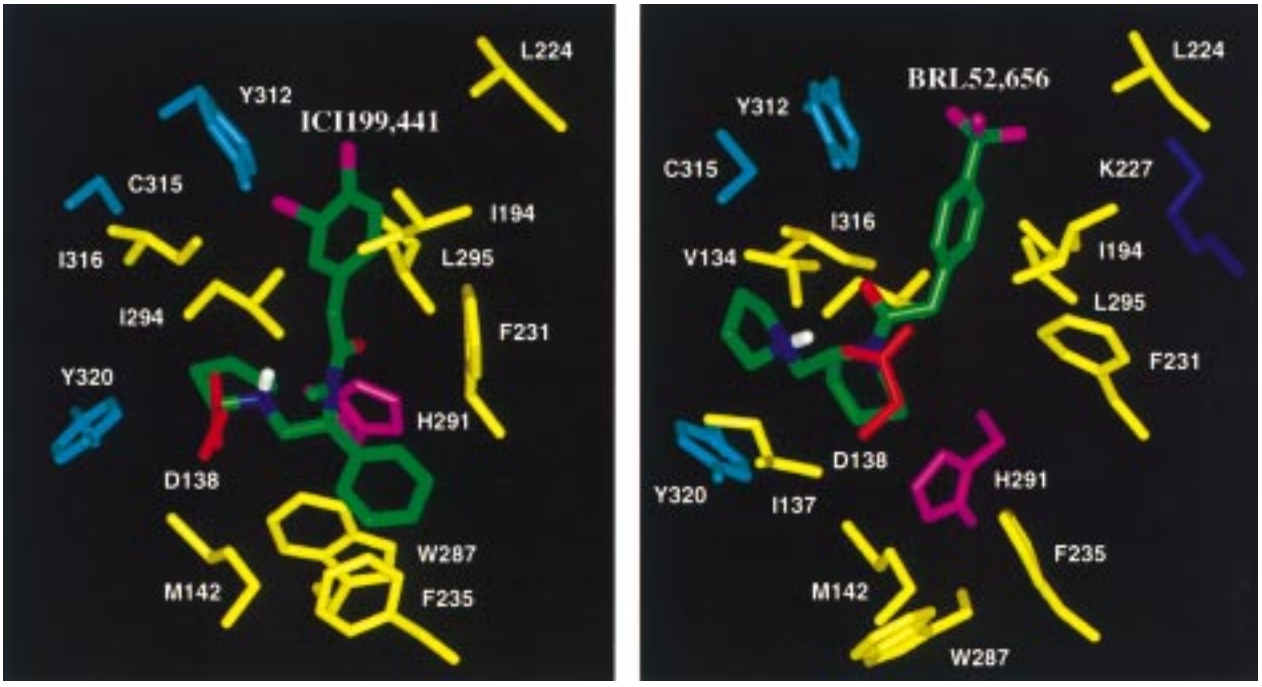

Figure 6. Molecular dynamics snapshot of ICI199,441−receptor (left) and BRL52,656−receptor (right) complexes. Selected residues that are within 5 Å from the ligands are shown as follows: D138 in red, polar residues in cyan, hydrophobic residues in yellow, and H291 in magenta.

Given the potential significance of this interaction in anchoring **1**−**10** to the κ-receptor, the quaternary pyrrolidine methiodide analogue (**14**) of **1** was prepared and evaluated for opioid agonist activity using the guinea pig ileum assay.[49] In contrast to **1,** which in the same assay exhibited an IC_{50} value of 7 nM, compound **14** showed little to no activity (20% response at 1 μM). Although **14** possesses a unit charge in common with that of **1**, the N-methylated pyrrolidine group apparently blocks the formation of a tight ion pair or salt link to D138. This was further verified by automated docking of **14** to the κ-receptor. The quaternary *N*-methyl group consistently docked 9−11 Å from D138, sterically hindering salt-link formation.

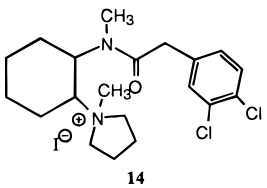

14

Among the other acidic residues in the TM helices (D105, D223, and E297), E297 in TM6 has been implicated in the binding of κ-antagonists such as norBNI.[50] However, the rather long distance between the ligands (**1**−**10**) and the carboxylate group of E297 (Table 5) rules out any possible nonbonded interaction. This interpretation is further supported by an experimental point mutation (E297A) that revealed the binding affinity of **5** and **7** to be less affected in the mutant receptor (Table 1). Of the other possible stabilizing receptor−ligand interactions, the carbonyl oxygen of U50,488 may form a H-bond with the histidyl (H291) N−H bond in TM6. Considering the δ-tautomer of H291 in the present study, automated docking of **1** disfavored such a nonbonded interaction as the corresponding (δ-H291)N−H···O═C(U50,488) distance was 7.4 Å on an average. A similar trend in the (δ-H291)N−H···O═C(ligand) interaction was evident for the bound complexes of **2**−**10**. Proximity of the ϵ-nitrogen in δ-H291 to the carbonyl oxygen (ϵN···O═C) in **6**−**8** indicated the likelihood of a weak H-bond, if the ϵ-tautomer (ϵ-H291) were considered. However, the influence of δ- or ϵ-H291 on ligand binding properties appears to be modest as revealed by site-directed mutagenesis. As opposed to the carbonyl group in **1**−**10**, the sp^3 oxygen in **3** and **5** (Figure 5) could form an H-bond with the N−H moiety in ϵ-H291 and influence the binding properties upon specific mutation. This explains the 7-fold decrease in CI-977 binding upon H291A mutation and perhaps the cause for the increased binding affinity of **5** over **2**.[7,11] Unlike the μ-receptor which displays significant loss in opiate agonist binding upon histidine mutation in TM6,[51] the present MD simulation results and available site-directed mutagenesis studies suggest that H291 is not involved directly in ligand binding or recognition in this series. This is not due to the lack of a hydroxyl substituent on the aryl group (to mimic the tyramine moiety in most opiate ligands) but is a consequence of the different binding orientations of the substituted arylacetamides (**1**−**10**) and the benzomorphan derivatives such as ethylketocyclazocine. The experimental K_i values of racemic **9** (0.5 nM), **10** (0.8 nM), and **13** (194.0 nM)[10] which differ only in the aryl substitution reveal that **13** with a hydroxyl substituent has a much weaker binding affinity than **9** and **10** which is consistent with our binding site model. Our proposed binding orientation for κ-agonists (**1**−**10**) is also supported by experimental results that illustrate sulfhydryl alkylating agents inhibit U50,488 binding,[52] thereby indicating the presence of a sulfhydryl group near the binding site. Consistently, the MD simulations captured C315 of TM7 close to the aryl group of **1**.

Apart from these specific point interactions, the κ-agonists are flanked by hydrophobic residues (Table 6) in the TM region. Consequently, mutation of any of these residues will have only a marginal effect on the ligand binding properties, since free rotation around the single bonds of the ligand and receptor side chains would allow torsional flexibility for the agonist to readjust to the mutated environment. For instance, the aryl group in **1**−**10** benefits from the hydrophobic interactions of I194, I294, L295, A298, and I316 residues. Even though a simple I294A mutation does not affect the κ-affinity (as in **5** and **7**), mutation to a charged residue (I294K) impairs CI-977 and ICI199,-441 binding significantly (Table 1). Despite the mutated residue (I294K) exerting similar effects on the binding profile of **5** and **7**, the subtle differences in the relative orientation of the ligands in the receptor may be responsible for the uneven deviation in the magnitude of the binding affinity.

Table 6. Key Residues Defining the κ-Opioid Receptor Pocket Involved in Agonist (**1**−**10**) Binding as Obtained from the Receptor−Ligand Snapshot (750-ps) Structure during the MD Simulation (κ-Receptor-Specific Residues are Underlined)

TM3:	V134,[a] I135, I137,[a] D138, Y139, M142
TM4:	W183,[b] A186,[b] G190,[b] I194
TM5:	L224, F231, V232,[a] A234,[a,b] F235
TM6:	W287, H291, I294, L295, E297,[c] A298
TM7:	Y312, C315, I316, A317, G319, Y320

[a] Involved additionally in **9** and **10**. [b] Involved additionally in **6**−**8**. [c] Not within 5-Å radii of **6**−**8**.

The cyclohexyl ring in **1**−**5**, the phenyl/isopropyl group in **6**−**8**, and the piperidine ring in **9** and **10** are also stabilized by nonpolar aromatic residues (F231, F235, and W287) and M142 with additional contributions from W183, A186, G190, and A234 for **6**−**8** and V232 and A234 for **9**, respectively. Likewise, the pyrrolidine ring in **1**−**10** benefits from the hydrophobic cooperation of I294, L295, I316, and G319 of the κ-receptor. In fact, the importance of G319 (TM7) in ligand binding has been demonstrated by site-directed mutagenesis studies (G319V) which weaken (by 28-fold) the binding affinity of **7**. Therefore, mutation of G319 with sterically bulkier groups should decrease the binding affinity of many other κ-agonists in this series. In addition, the involvement of polar residues such as Y139, Y312, and Y320 that are also part of the ligand binding pocket can be probed by appropriate receptor mutations.

Another test of the proposed docking mode can be found in the enantioselectivity of the κ-agonists for the receptor. As the carboxylate group of D138 and the N−H bond in **1**−**10** may be involved in direct receptor−ligand interaction, any change in the ligand orientation (θ_5) around this region should destabilize κ-agonist binding. Thus, the enantiomers of **1**−**10** possessing a gauche$^+$ form for the θ_5 torsion (by mirror symmetry of the ligands) orient the proton on the basic nitrogen away from D138 leading to a very weak binding. This was demonstrated by docking the less active isomer (*R*,*R*)-**1** (K_i = 299 nM)[22] following the DOCK protocol described above. Out of the 144 best-docked configurations retrieved from a total of 1027 orientations, none had the N−H bond of (*R*,*R*)-**1** pointing toward the carboxylate group of D138. The corresponding distance ranges from 7 to 11 Å for most of the docked configurations and is obviously too far away for any possible ion-pairing or electrostatic interaction. The same reasoning can be extended to explain the enantioselective binding of other κ-agonists in this series.

Conclusion

In conclusion, the present study has revealed striking similarities in the three-dimensional structure, dynamics, and binding modes of representative arylacetamide κ-agonists. The SPASMS relative energy trends of **1**−**10** display systematic conformational preferences and show overall agreement throughout this ligand series. The

MD conformational sampling of **1** was consistent with the conformations derived from X-ray crystal data and from NMR experiments, justifying the reliability of the simulation results for other κ-ligands in this series. In addition, the simulations have also revealed that bicyclic aromatics reduce the θ_2 torsional flexibility and indicate possible leads for designing rigid κ-agonists (for example, bicyclic aromatics in **6**−**10**).

As was evident from the automated docking procedure and MD simulations of the receptor−agonist complex, the binding orientations of **1**−**10** differed from that of the opiates. Even though the protonated nitrogen of the non-peptide agonists associated with the κ-opioid receptor through ion pairing with the aspartate in TM3, the aryl ring in **1**−**10** does not mimic the binding environment of the phenolic component of the tyramine moiety of the opiate ligands. Thus, the histidine in TM6 (H291) which may form "hydrogen bonds" with the hydroxyl substituent on the phenolic moiety in many benzomorphan derivatives is not involved in any similar interaction with the ligand atoms in this series. Since the cyclohexyl ring in **1**−**5** and the ethyl spacer in **6**−**10** are close to H291 (Figures 5 and 6), incorporation of functional groups containing electronegative atoms in this region would provide insights into the role of H291 toward ligand binding. We should point out that an alternative role for H291 has been proposed in U50,488 binding by Cappelli et al.[53] While details of the molecular conformation and docking mode were not given in that paper, some differences in the receptor−ligand complex are evident, mainly in the orientation of H291 toward the carbonyl oxygen of U50,488. The binding site analysis of CI-977 and related ligands presented above, however, supports an alternative role for this proton donor. Nevertheless, such an interaction cannot be entirely ruled out given the proximity of H291 to the ligand binding site. The binding site model presented here also reveals several residues specific to the κ-receptor that may be useful in ligand design. Although D223 and E297 residues are apparently not involved in ligand binding of arylacetamides, they are viable sites that could reinforce the receptor−ligand association. Appropriate substituents (like guanidine) attached to the meta/para positions of the aromatic ring presumably may reach the acidic residues to increase the ligand binding affinity.

In addition to the key electrostatic interaction stabilizing the receptor−agonist complex, the results indicate a network of surrounding hydrophobic residues that may strengthen ligand binding in this series. Nearly one-third of the residues involved in ligand binding are unique to the κ-receptor, which may explain the differential μ/κ-selectivity of the U50,488 derivatives. This suggests a very different mechanism of recognition when compared with the κ-opioid antagonist norBNI. Previous computational and experimental studies of norBNI binding to the κ-receptor have indicated E297 (near the top of TM6) to be critical to selectivity.[50] Our structural analysis, however, shows this acidic residue plays no part in U50,488 binding as noted above. While our model is consistent with available site-directed mutagenesis data, additional work is needed to fully define this putative binding pocket and how it differs from that of the μ- and δ-receptors.

Finally, it is important to point out that the results strongly support the existence of multiple binding epitopes for opioid receptors. In comparing the analysis presented here with previous docking studies involving opiates and peptides, divergent models of recognition and selectivity emerge.[6,24] Although this further complicates both receptor and ligand modeling efforts, knowledge of additional recognition sites within the μ-, δ-, or κ-opioid receptors may lend new insight to the development of even more potent and selective ligands. Moreover, such sites may provide important clues as to the structural basis of agonist versus antagonist recognition that would have a far reaching impact on GPCR research.

Acknowledgment. The authors thank NIH/NIDA for financial support to D.M.F. and P.S.P. and Dr. Thue Schwartz for sharing his site-directed mutagenesis results.

Supporting Information Available: Fragmentation scheme used for deriving RESP atomic charges; tables of experimental K_i/IC_{50} values; SPASMS conformational energies of **2**−**10**; in vacuo geometry-optimized coordinates (PDB format) and MD simulation profiles of the solvated and docked ligands, along with the putative ligand binding pocket and binding orientations generated from the automated docking procedure; and experimental details and characterization of **14** (28 pages). Ordering information is given on any current masthead page.

References

(1) (a) Martin, W. R. Pharmacology of Opioids. *Pharmacol. Rev.* **1983**, *35*, 283−323. (b) Millan, M. J. Multiple Opioid Systems and Pain. *Pain* **1986**, *27*, 303−347. (c) Jaffe, J. H.; Martin, W. R. Opioid Analgesics and Antagonists. In *The Pharmacological Basis of Therapeutics*, 8th ed.; Gilman, A. G., Rall, T. W., Nies, A. S., Taylor, P., Eds.; Pergamon Press: New York, 1990; pp 485−521. (d) Satoh, M.; Minami, M. Molecular Pharmacology of the Opioid Receptors. *Pharmacol. Ther.* **1995**, *68*, 343−364. (e) Kieffer, B. L. Recent Advances in Molecular Recognition and Signal Transduction of Active Peptides: Receptors for Opioid Peptides. *Cell. Mol. Neurobiol.* **1995**, *15*, 615−635.

(2) (a) Olson, G. A.; Olson, R. D.; Kastin, A. J.; Coy, D. H. Endogenous Opiates: 1981. *Peptides* **1982**, *3*, 1039−1072. (b) Römer, D.; Buscher, H. H.; Hill, R. C.; Maurer, R.; Petcher, T. J.; Zeugner, H.; Benson, W.; Finner, E.; Milkowsky, W.; Thies, P. W. An Opioid Benzodiazepine. *Nature (London)* **1982**, *298*, 759−760. (c) Römer, D.; Buscher, H. H.; Hill, R. C.; Maurer, R.; Petcher, T. J.; Zeugner, H.; Benson, W.; Finner, E.; Milkowsky, W.; Thies, P. W. Unexpected Opioid Activity in a Known Class of Drug. *Life Sci.* **1982**, *31*, 1217−1220. (d) Kley, H.; Scheidemantel, U.; Bering, B.; Muller, W. E. Reverse Stereoselectivity of Opiate and Benzodiazepine Receptors for the Opioid Benzodiazepine Trifluadom. *Eur. J. Pharmacol.* **1983**, *87*, 503−504. (e) Wood, P. L. Opioid Receptor Affinities of Kappa Agonists, Agonist/Antagonists and Antagonists In Vitro and In Vivo. *Prog. Neuro-Psychopharmacol. Biol. Psychiatry* **1983**, *7*, 657−662. (f) Dhawan, B. N.; Cesselin, F.; Raghubir, R.; Reisine, T.; Bradley, P. B.; Portoghese, P. S.; Hamon, M. International Union of Pharmacology. XII. Classification of Opioid Receptors. *Pharmacol. Rev.* **1996**, *48*, 567−592.

(3) (a) Szmuszkovicz, J.; von Voigtlander, P. F. Benzeneacetamide Amines: Structurally Novel Non-μ Opioids. *J. Med. Chem.* **1982**, *25*, 1125−1126. (b) Lahti, R. A.; von Voigtlander, P. F.; Barsuhn, C. Properties of a Selective Kappa Agonist, U-50,488H. *Life Sci.* **1982**, *31*, 2257−2260. (c) von Voigtlander, P. F.; Lahti, R. A.; Ludens, J. H. U-50,488: A Selective and Structurally Novel Non-Mu (Kappa) Opioid Agonist. *J. Pharmacol. Exp. Ther.* **1983**, *224*, 7−12. (d) de Costa, B. R.; Bowen, W. D.; Hellewell, S. B.; George, C.; Rothman, R. B.; Reid, A. A.; Walker, J. M.; Jacobson, A. E.; Rice, K. C. Alterations in the Stereochemistry of the κ-Selective Opioid Agonist U50,488 Result in High-Affinity σ Ligands. *J. Med. Chem.* **1989**, *32*, 1996−2002.

(4) Bellucci, F.; Dondio, G. Molecular Modelling Comparison of Potent and Selective κ Agonists Belonging to Different Chemical Structures: A First Attempt to κ Receptor Mapping. In *Trends*

in QSAR and Molecular Modeling '92; Proceedings of the 9th European Symposium on Structure−Activity Relationships: QSAR and Molecular Modeling; Vermuth, C. G., Ed.; ESCOM: Leiden, 1993; pp 461−462.

(5) (a) Portoghese, P. S.; Nagase, H.; Lipkowski, A. W.; Larson, D. L.; Takemori, A. E. Binaltorphimine-Related Bivalent Ligands and Their κ-Opioid Receptor Antagonist Selectivity. *J. Med. Chem*. **1988**, *31*, 836−841. (b) Takemori, A. E.; Portoghese, P. S. Selective Naltrexone-Derived Opioid Receptor Antagonists. *Annu. Rev. Pharmacol. Toxicol*. **1992**, *32*, 239−269. (c) Lomize, A. L.; Pogozheva, I. D.; Mosberg, H. I. Development of a Model for the δ-Opioid Receptor Pharmacophore: 3. Comparison of the Cyclic Tetrapeptide, tyr-c[D-Cys-Phe-D-Pen]OH with other conformationally Constrained δ-Receptor Selective Ligands. *Biopolymers* **1996**, *38*, 221−234.

(6) Metzger, T. G.; Paterlini, M. G.; Portoghese, P. S.; Ferguson, D. M. Application of the Message-Address Concept of the Docking of Naltrexone and Selective Naltrexone-Derived Opioid Antagonists into Opioid Receptor Models. *Neurochem. Res*. **1996**, *21*, 1287−1294.

(7) Halfpenny, P. R.; Hill, R. G.; Horwell, D. C.; Hughes, J.; Hunter, J. C.; Johnson, S.; Rees, D. C. Highly Selective κ-Opioid Analgesics. 2. Synthesis and Structure−Activity Relationships of Novel N-[(2-Aminocyclohexyl)aryl]acetamide Derivatives. *J. Med. Chem*. **1989**, *32*, 1620−1626.

(8) Halfpenny, P. R.; Horwell, D. C.; Hughes, J.; Hunter, J. C.; Rees, D. C. Highly Selective κ-Opioid Analgesics. 3. Synthesis and Structure−Activity Relationships of Novel N-[2-(1-Pyrrolidinyl)-4- or -5-substituted-cyclohexyl]arylacetamide Derivatives. *J. Med. Chem*. **1990**, *33*, 286−291.

(9) Hayes, A. G.; Birch, P. J.; Hayward, N. J.; Sheehan, M. J.; Rogers, H.; Tyers, M. B.; Judd, D. B.; Scopes, D. I. C.; Naylor, A. A series of Novel, Highly Potent and Selective Agonists for the κ-Opioid Receptor. *Br. J. Pharmacol*. **1990**, *101*, 944−948.

(10) Vecchietti, V.; Giordani, A.; Giardina, G.; Colle, R.; Clarke, G. D. (2S)-1-(Arylacetyl)-2-(aminomethyl)piperidine Derivatives: Novel, Highly Selective κ Opioid Analgesics. *J. Med. Chem*. **1991**, *34*, 397−403.

(11) Giardina, G.; Clarke, G. D.; Dondio, G.; Petrone, G.; Sbacchi, M.; Vecchietti, V. Selective κ-Opioid Agonists: Synthesis and Structure−Activity Relationships of Piperidines Incorporating an Oxo-Containing Acyl Group. *J. Med. Chem*. **1994**, *37*, 3482−3491.

(12) Vecchietti, V.; Clarke, G. D.; Colle, R.; Giardina, G.; Petrone, G.; Sbacchi, M. (1S)-1-(Aminomethyl)-2-(arylacetyl)-1,2,3,4-tetrahydroisoquinoline and Heterocyclic-Condensed Tetrahydropyridine Derivatives: Members of a Novel Class of Very Potent κ Opioid Analgesics. *J. Med. Chem*. **1991**, *34*, 2624−2633.

(13) Clark, C. R.; Halfpenny, P. R.; Hill, R. G.; Horwell, D. C.; Hughes, J.; Jarvis, T. C.; Rees, D. C.; Schofield, D. Highly Selective κ Opioid Analgesics. Synthesis and Structure−Activity Relationships of Novel N-[(2-Aminocyclohexyl)aryl]acetamide and N-[(2-Aminocyclohexyl)aryloxy]acetamide Derivatives. *J. Med. Chem*. **1988**, *31*, 831−836.

(14) Lahti, R. A.; Mickelson, M. M.; McCall, J. M.; von Voigtlander, P. F. [^{3}H]U-69593 A Highly Selective Ligand for the Opioid κ Receptor. *Eur. J. Pharmacol*. **1985,** *109*, 281−284.

(15) (a) von Voigtlander, P. F.; Lewis, R. A. Analgesic and Mechanistic Evaluation of Spiradoline, a Potent Kappa Opioid. *J. Pharmacol. Exp. Ther*. **1988**, *246*, 259−262. (b) Meecham, K. G.; Boyle, S. J.; Hunter, J. C.; Hughes, J. An in vitro Profile of Activity for the (+) and (−) Enantiomers of Spiradoline and PD117302. *Eur. J. Pharmacol*. **1989**, *173*, 151−157.

(16) Hunter, J. C.; Leighton, G. E.; Meecham, K. G.; Boyle, S. J.; Horwell, D. C.; Rees, D. C.; Huges, J. CI-977, a Novel and Selective Agonist for the κ-Opioid Receptor. *Br. J. Pharmacol*. **1990**, *101*, 183−189.

(17) Weerawarna, S. A.; Davis, R. D.; Nelson, W. L. Isothiocyanate-Substituted κ-Selective Opioid Receptor Ligands Derived from *N*-Methyl-N-[(1S)-1-phenyl-2-(1-pyrrolidinyl)ethyl]phenylacetamide. *J. Med. Chem*. **1994**, *37*, 2856−2864.

(18) Costello, G. F.; Main, B. G.; Barlow, J. J.; Carroll, J. A.; Shaw, J. S. A Novel Series of Potent and Selective Agonists at the Opioid κ-Receptor. *Eur. J. Pharmacol*. **1988**, *151*, 475−478.

(19) (a) Nock, B.; Giordano, A. L.; Cicero, T. J. ICI 197067 is a Selective Ligand for the U-69593-sensitive κ Opiate Binding Site. *Eur. J. Pharmacol*. **1989**, *162*, 385−386. (b) Shaw, J. S.; Carroll, J. A.; Alcock, P.; Main, B. G. ICI 204448: a κ-Opioid Agonist with Limited Access to the CNS. *Br. J. Pharmacol*. **1989**, *96*, 986−992.

(20) Barlow, J. J.; Blackburn, T. P.; Costello, G. F.; James, R.; Le Count, D. J.; Main, B. G.; Pearce, R. J.; Russell, K.; Shaw, J. S. Structure/Activity Studies Related to 2-(3,4-Dichlorophenyl)-*N*-methyl-N-[2-(1-pyrrolidinyl)-1-substituted-ethyl]acetamides: A Novel Series of Potent and Selective κ-Opioid Agonists. *J. Med. Chem*. **1991**, *34*, 3149−3158.

(21) Naylor, A.; Judd, D. B.; Lloyd, J. E.; Scopes, D. I. C.; Hayes, A. G.; Birch, P. J. A Potent New Class of κ-Receptor Agonist: 4-Substituted 1-(Arylacetyl)-2-[(dialkylamino)methyl]piperazines. *J. Med. Chem*. **1993**, *36*, 2075−2083.

(22) (a) Rothman, R. B.; Bykov, V.; Reid, A.; de Costa, B. R.; Newman, A.-H.; Jacobson, A. E.; Rice, K. C. A Brief Study of the Selectivity of Norbinaltorphimine, (−)-Cyclofoxy, and (+)-Cyclofoxy Among Opioid Receptor Subtypes In Vitro. *Neuropeptides* **1988**, *12*, 181−187. (b) Rothman, R. B.; France, C. P.; Bykov, V.; de Costa, B. R.; Jacobson, A. E.; Woods, J. H.; Rice, K. C. Pharmacological Activities of Optically Pure Enantiomers of the κ-Opioid Agonist, U50,488, and its cis Diastereomer: Evidence for Three κ Receptor Subtypes. *Eur. J. Pharmacol*. **1989**, *167*, 345−353.

(23) Costello, G. F.; James, R.; Shaw, J. S.; Slater, A. M.; Stutchbury, N. C. J. 2-(3,4-Dichlorophenyl)-*N*-methyl-N-[2-(1-pyrrolidinyl)-1-substituted-ethyl]acetamides: The Use of Conformational Analysis in the Development of a Novel Series of Potent Opioid κ Agonists. *J. Med. Chem*. **1991**, *34*, 181−189.

(24) Paterlini, G.; Portoghese, P. S.; Ferguson, D. M. Molecular Simulation of Dynorphin A(1−10) Binding to Extracellular Loop 2 of the κ-Opioid Receptor. A Model for Receptor Activation. *J. Med. Chem*. **1997**, *40*, 3254−3262.

(25) Kong, H.; Raynor, K.; Reisine, T. Amino Acids in the Cloned Mouse Kappa Receptor that are Necessary for High Affinity Agonist Binding but not Antagonist Binding. *Reg. Pept*. **1994**, *54*, 155−156.

(26) (a) Thirstrup, K.; Elling, E. C.; Hjorth, S. A.; Schwartz, T. W. Construction of a High Affinity Zinc Switch in the κ-Opioid Receptor. *J. Biol. Chem*. **1996**, *271*, 7875−7878. (b) Hjorth, S. A.; Thirstrup, K.; Schwartz, T. W. Radioligand-dependent Discrepancy in Agonist Affinities Enhanced by Mutations in the κ-Opioid Receptor. *Mol. Pharmacol*. **1996**, *50*, 977−984.

(27) (a) Doi, M.; Ishida, T.; Inoue, M. Structure of κ-Agonist, U-50488 *Acta Crystallogr*. **1990**, *C46*, 676−678. (b) Doi, M.; Ishida, T.; Inoue, M. Conformational Characteristics of Opioid κ-receptor agonist: Crystal Structure of (5S,7S,8S)−(−)*N*-Methyl-N-[7-(1-pyrrolidinyl)-1-oxaspiro[4.5]dec-8-yl)benzeneacetamide (U69,-593), and Conformational Comparison with κ-Agonists. *Chem. Pharm. Bull*. **1990**, *38*, 1815−1818. (c) Chang, A.-C.; Takemori, A. E.; Ojala, W. H.; Gleason, W. B.; Portoghese, P. S. κ Opioid Receptor Selective Affinity Labels: Electrophilic Benzeneacetamides as κ-Selective Opioid Antagonists. *J. Med. Chem*. **1994**, *37*, 4490−4498.

(28) Cieplak, P.; Cornell, W. D.; Bayly, C.; Kollman, P. A. Application of the Multimolecule and Multiconformational RESP Methodology to Biopolymers: Charge Derivation for DNA, RNA, and Proteins. *J. Comput. Chem*. **1995**, *16*, 1357−1377.

(29) (a) Pearlman, D. A.; Case, D. A.; Caldwell, J. W.; Ross, W. S.; Cheatham, T. E., III; Debolt, S.; Ferguson, D. M.; Seibel, G. L.; Kollman, P. A. AMBER, a Package of Computer Programs for Applying Molecular Mechanics, Normal-Mode Analysis, Molecular Dynamics and Free Energy Calculations to Simulate the Structural and Energetic Properties of Molecules. *Comput. Phys. Commun*. **1995**, *91*, 1−41. (b) Pearlman, D. A.; Case, D. A.; Caldwell, J. W.; Ross, W. S.; Cheatham, T. E., III; Ferguson, D. M.; Seibel, G. L.; Singh, U. C.; Weiner, P. K.; Kollman, P. A. AMBER, Version 4.1; Department of Pharmaceutical Chemistry, University of California: San Francisco, CA, 1995.

(30) Cornell, W. D.; Cieplak, P.; Bayly, C. I.; Gould, I. R.; Merz, K. M., Jr.; Ferguson, D. M.; Spellmeyer, D. C.; Fox, T.; Caldwell, J. W.; Kollman, P. A. A Second Generation Force Field for the Simulation of Proteins, Nucleic Acids, and Organic Molecules. *J. Am. Chem. Soc*. **1995**, *117*, 5179−5197.

(31) Jorgensen, W. L.; Chandrasekhar, J.; Madura, J. D.; Impey, R. W.; Klein, M. L. Comparison of Simple Potential functions for Simulating Liquid Water. *J. Chem. Phys*. **1983**, *79*, 926−935.

(32) Berendsen, H. J. C.; Postma, J. P. M.; van Gunsteren, W. F.; DiNola, A.; Haak, J. R. Molecular Dynamics with Coupling to an External Bath. *J. Chem. Phys*. **1984**, *81*, 3684−3690.

(33) (a) Meng, E. C.; Shoichet, B. K.; Kuntz, I. D. Automated Docking with Grid-Based Energy Evaluation. *J. Comput. Chem*. **1992**, *13*, 505−524. (b) Meng, E. C.; Gschwend, D. A.; Blaney, J. M.; Kuntz, I. D. Orientational Sampling and Rigid-Body Minimization in Molecular Docking. *Proteins: Struct. Funct. and Genet*. **1993**, *17*, 266−278. (c) Connolly, M.; Gschwend, D. A.; Good, A. C.; Oshiro, C.; Kuntz, I. D. DOCK, Version 3.5; Department of Pharmaceutical Chemistry, University of California: San Fransisco, CA, 1995.

(34) Baldwin, J. M.; Schertler, G. F. X.; Unger, V. M. An Alpha-carbon Template for the Transmembrane helices in the Rhodopsin Family of G-protein-coupled Receptors. *J. Mol. Biol*. **1997**, *272*, 144−164.

(35) Xue, J. C.; Chen, C.; Zhu, J.; Kunapuli, S.; DeRiel, J. K.; Yu, L.; Liu-Chen, L.-Y. Differential Binding Domains of Peptide and Non-peptide Ligands in the Cloned Rat κ-opioid Receptor. *J. Biol. Chem*. **1994**, *269*, 30195−30199.

(36) (a) Connolly, M. L. Solvent-Accessible Surfaces of Proteins and Nucleic Acids. *Science* **1983**, *221*, 709−713. (b) Connolly, M. L. Analytical Molecular Surface Calculation. *J. Appl. Crystallogr.* **1983**, *16*, 548−558.

(37) Molecular Graphics Images were produced using the MidasPlus Program from the Computer Graphics Laboratory, University of California, San Fransisco (supported by NIH RR-01081). Ferrin, T. E.; Huang, C. C.; Jarvis, L. E.; Langridge, R. The MIDAS Display System. *J. Mol. Graph.* **1988**, *6*, 13−27.

(38) Young, L.; Topol, I. A.; Rashin, A. A.; Burt, S. K. Building Molecular Charge Distributions from Fragments: Application to HIV-1 Protease Inhibitors. *J. Comput. Chem.* **1997**, *18*, 522−532 and references therein.

(39) Foresman, J. B.; Frisch, Æ. *Exploring Chemistry with Electronic Structure Methods*, 2nd ed.; Gaussian, Inc.: Pittsburgh, 1996.

(40) Frisch, M. J.; Trucks, G. W.; Schlegel, H. B.; Gill, P. M. W.; Johnson, B. G.; Robb, M. A.; Cheeseman, J. R.; Keith, T.; Petersson, G. A.; Montgomery, J. A.; Raghavachari, K.; Al-Laham, M. A.; Zakrzewski, V. G.; Ortiz, J. V.; Foresman, J. B.; Cioslowski, J.; Stefanov, B. B.; Nanayakkara, A.; Challacombe, M.; Peng, C. Y.; Ayala, P. Y.; Chen, W.; Wong, M. W.; Andres, J. L.; Replogle, E. S.; Gomperts, R.; Martin, R. L.; Fox, D. J.; Binkley, J. S.; Defrees, D. J.; Baker, J.; Stewart, J. J. P.; Head-Gordon, M.; Gonzalez, C.; Pople, J. A. Gaussian 94, Revision E2; Gaussian, Inc.: Pittsburgh, PA, 1995.

(41) Allinger, N. L. Conformational Analysis. 131. MM2. A Hydrocarbon Force Field Utilizing V_1 and V_2 Torsional Terms. *J. Am. Chem. Soc.* **1977**, *99*, 8127−8134; subsequent versions, e.g., MM2-87, MM2-89, MM2-91.

(42) Veenstra, D. L.; Ferguson, D. M.; Kollman, P. A. How Transferable are Hydrogen parameters in Molecular Mechanics Calculations? *J. Comput. Chem.* **1992**, *13*, 971−978.

(43) Froimowitz, M.; DiMeglio, C. M.; Makriyannis, A. Conformational Preferences of the κ-Selective Opioid Agonist U50488. A Combined Molecular Mechanics and Nuclear Magnetic Resonance Study. *J. Med. Chem.* **1992**, *35*, 3085−3094.

(44) Cheng, C.-Y.; Lu, H.-Y.; Lee, F.-M.; Tam, S. W. Synthesis of (1′,2′-trans)-3-Phenyl-1-[2′-(N-pyrrolidinyl)cyclohexyl]pyrrolid-2-ones as κ-Selective Opiates. *J. Pharm. Sci.* **1990**, *79*, 758−762.

(45) Strahs, D.; Weinstein, H. Comparative Modeling and Molecular Dynamics Studies of the δ, κ, and μ Opioid Receptors. *Protein Eng.* **1997**, *10*, 1019−1038.

(46) (a) Thirstrup, K.; Hjorth, S. A.; Schwartz, T. W. Investigation of the Binding Pocket in the Kappa Opioid Receptor by a Combination of Alanine Substitutions and Steric Hindrance Mutagenesis. *27*th Meeting of the International Narcotics Research Conference (INRC) ′96, 1996; poster M30. (b) Thirstrup, K.; Hjorth, S. A.; Schwartz, T. W. Unpublished results.

(47) Independent automated docking of **2**−**8** following the standard DOCK protocols discussed in the text also revealed the binding orientation of these ligands to be similar to that of **1**.

(48) (a) Barlow, D. J.; Thornton, J. M. Ion-Pairs in Proteins. *J. Mol. Biol.* **1983**, *168*, 867−885. (b) Zheng, Y.-J.; Ornstein, R. L. What Happens to Salt-Bridges in Nonaqueous Environments: Insights from Quantum Mechanics Calculations. *J. Am. Chem. Soc.* **1996**, *118*, 11237−11243 and references therein.

(49) Rang, H. P. Stimulant Actions of Volatile Anaesthetics on Smooth Muscle. *Br. J. Pharmacol.* **1964**, *22*, 356−365.

(50) Hjorth, S. A.; Thirstrup, K.; Grandy, D. K.; Schwartz, T. W. Analysis of Selective Binding Epitopes for the κ-Opioid Receptor Antagonist Nor-binaltorphimine. *Mol. Pharmacol.* **1995**, *47*, 1089−1094.

(51) Spivak, C. E.; Beglan, C. L.; Seidleck, B. K.; Hirshben, L. D.; Blaschak, C. J.; Uhl, G. R.; Surratt, C. K. Naloxone Activation of μ-Opioid Receptors Mutated at a Histidine Residue Lining the Opioid Binding Cavity. *Mol. Pharmacol.* **1997**, *52*, 983−992 and references therein.

(52) Joseph, D. B.; Bidlack, J. M. The κ-Opioid Receptor Expressed on the Mouse Lymphoma Cell Line R1.1 Contains a Sulfhydryl Group at the Binding Site. *Eur. J. Pharmacol.* **1994**, *267*, 1−6.

(53) Cappelli, A.; Anzini, M.; Vomero, S.; Menziani, M. C.; De Benedetti, P. G.; Sbacchi, M.; Clarke, G. D.; Mennuni, L. Synthesis, Biological Evaluation, and Quantitative Receptor Docking Simulations of 2-[(Acylamino)ethyl]-1,4-benzodiazepines as Novel Tifluadom-like Ligands with High Affinity and Selectivity for κ-Opioid Receptors. *J. Med. Chem.* **1996**, *39*, 860−872.

JM9803166